Journal of Theoretical
and Applied Mechanics
Sofia, 1992, Year XXIII, No 2

V. V o l l e r,
C. S w a m i n a t h a n

Fixed Grid Solution of Phase Change Problems

Introduction

A basic example of phase change system involves the conduction controlled solidification (or melting) of a pure metal. Such a system is characterized by the movement of the solid/liquid phase interface at which an energy balance (the Stefan condition [1]) needs to be satisfied. There are few analytical solutions for these systems [1]. A vast array of numerical solutions, however, have been developed over the past four decades [1]. Broadly speaking, numerical solutions can be placed into two classes:

1. those that attempt to track the moving interface using an adaptive grid.
2. those based on a numerical grid which is fixed in space. In the former case, the required energy balance on the moving boundary is readily incorporated into the numerical scheme. In the latter case, account of the energy balance at the interface is made on solving in terms of a conserved variable (i.e., the enthalpy).

General solidification systems are more complicated than the basic case outlined before. Typically the phase change (the evolution of the latent heat) will occur over a range of temperatures as apposed to a single temperature. This in turn will lead to a solid/liquid mushy region as opposed to a sharp solid/liquid interface. Further the morphology of this mushy region can take a number of possible forms ranging from columnar crystals to free floating equal-axed grains [2]. A schematic of the mushy region illustrating the possible morphologies is given in Fig.1. Modelling of such systems could involve the coupled solution of heat, mass and solute transport along with the appropriate interaction with the mushy region morphology [3-5]. Due to the strong coupling and interactions, such systems can be solved numerically only on a fixed space grid. The key elements in such a solution is solving for the fluid flow and the latent heat evolution. In terms of modelling the fluid flow, the well

established algorithms (e.g. pressure correction control volumes [6], SUPG finite elements [7]) can be used. The requirement in such cases is the correct modelling of the physical nature of the solidification, in particular the impact of the morphology and behaviour of the solid/liquid mushy region on the flow. A common approach is to arrive at a single momentum equation which is valid throughout the domain. This is achieved on the inclusion of appropriate source terms, e.g., a Darcy like source term to represent the porous nature of the mushy region. A range of examples of this approach can be found in references [3-5]. This paper will concentrate on numerical approaches for dealing with the evolution of latent heat. Towards this end, it will be assumed that a velocity field can be obtained from the solution of appropriate hydromechanic equations and as such only numerical solutions of the heat transport equation will be considered.

Governing equation

In modelling solidification phase change systems it is always important to recognize the two phase nature of the system. Typically the system will consist of a fully solid phase, a solid/liquid mushy phase, and a fully liquid phase, see Fig.1. Following Voller et al [5] a single domain equation can be obtained on summing the appropriate two phase equations

$$(1) \qquad \frac{\partial}{\partial t}(\rho H) + \nabla.\,[\rho_l g\, u_l\, H_l + \rho_s (1-g)\, u_s\, H_s] = \nabla.\,(K \nabla T)$$

where T is the temperature, g is a volume liquid fraction, and the subscripts s and 1 refer to solid and liquid phase respectively.

$$\rho H = \rho_s (1 - g) H_s + \rho_l g H_l$$

defines a mixture enthalpy in terms of the phase enthalpies, and

$$K = g K_s + (1 - g) K_l$$

is a mixture conductivity. In a numerical context Eq.(1) is potentially convenient because it will allow for a numerical discretization on a fixed space grid (finite difference or finite element).

Equations for specific solidification systems

At this point it is worthwhile to write down versions of Eq.(1) which are appropriate for various solidification systems.

Case a: A static casting with a collumnar dendritic mushy region - In this system the solid velocity $u_s = 0$ and a system velocity can be defined as $u = f u_l$ where f is the local liquid mass fraction, i.e., $\rho f = \rho_l g$. With the given definitions, Eq.(1) becomes

$$(2) \qquad \frac{\partial}{\partial t}(\rho H) + V.[p\ u\ H_l] = \nabla.(K \nabla T)$$

Case b: A static casting with equi-axed mushy region - If the free floating equi-axed grains are assumed to be moving with the fluid velocity $u_s = u_l = u$ then Eq.(1) becomes

$$(3) \qquad \frac{\partial}{\partial t}(\rho H) + \nabla.[\rho\ u\ H] = \nabla.(K \nabla T)$$

On comparing Eq.(2) and Eq.(3), it should be remembered that the definition of the system velocity u is different in each case and that the convection term in Eq.(2) is in terms of the liquid phase enthalpy and not the mixture enthalpy as in Eq.(3). This apparently small change can lead to quite different results [8].

A general implicit solution

After an appropriate fixed grid space discretization of the above equations one would like to seek an implicit time integrated solution. This is primarily motivated by stability and efficiency requirements. A major problem in obtaining an implicit solution is the fact that the governing equations are written in terms of two dependent variables (enthalpy H and temperature T). In some systems the definitions of thermal properties is such that the major components in the equation (i.e., the transient, convective and diffusive terms) can be written down in terms of a single variable (enthalpy H [9], sensible enthalpy h [5], or temperature T [10]) along with a source term accounting for latent heat evolution written in terms of the local liquid fraction. A successful solution approach based on liquid fraction source formulations can be found in Voller and Swaminathan [11]. The drawback to the approach is that it is not always possible to identify a suitable liquid fraction temperature relationships. In this paper a more recent general approach will be presented [12]. This approach has many similarities to the liquid fraction source method but only requires that the enthalpy is specified in terms of temperature, i.e., H = G(T). In outlining this technique we take Eq.(2) as an example. The system of equations resulting from a fully implicit time discretization of this equation can be represented by the point equation

$$(5) \qquad a_p T_p^{m+1} = \sum_{nb} a_{nb} T_{nb}^{m+1} + d_p (H_p^{old} - H_p^{m+1}) - a_p^* [H_l]_p^{m+1} + \sum_{nb} a_{nb}^* [H_l]_p^{m+1}$$

Note that in this equation the "a" coefficients are formed from the diffusion term, the "d" coefficient from the transient term, and the "a"* from the convective term. As written this equation is highly non-linear. On employing a Taylor expansion approach the enthalpies can be expanded as

$$(6) \qquad H_p^{m+1} = H_p^m + \left.\frac{dH}{dT}\right|_{H_p^m} (T_p^{m+1} - G^{-1}(H_p^m))$$

and

$$(7) \qquad [H_1]_p^{m+1} = [H_1]_p^m + \left.\frac{dH_1}{dT}\right|_{[H_1]_p^m} (T_p^{m+1} - G_1^{-1}([H_1]_p^m))$$

The derivative dH/dT is replaced by an arbitrary large value at step discontinuities. These equations can be readily written in the form $S_p T_p + S_S$, which on substitution into Eq.(6) results in

$$(8) \quad a_p^+ T_p^{m+1} = \sum_{nb} a_{nb}^+ T_{nb}^{m+1} + d_p(H_p^{old} - [S_c]_p) - a_p^* [S_C^1]_p + \sum_{nb} a_{nb}^* [S_C^1]_p$$

Note that the coefficients marked with a "+" subscript have been augmented by the S_p terms. During a given iteration, the coefficients used in Eq.(8) and the components of the source terms, S_p and S_C are calculated from the enthalpy fields H^m and H_1^m. The system of equations defined by Eq.(8) is then solved for the temperature field T^{m+1}. Following this step the $m+1^{th}$ enthalpy fields are updated in a point wise fashion from Eq.(6) and Eq.(7). This iteration pattern continues to convergence.

Examples

In this section we consider three test examples. The first two examples are conduction driven solidification problems while the third example involves the solution of the coupled Navier-Stokes and the energy equation during the melting of pure gallium.

Solidification of an Al-4.5% Cu alloy - We consider the solidification of an Al-4.5% Cu alloy initially at a uniform temperature of 969 K (greater than the liquidus temperature). The enthalpy variation with temperature follows the Scheil equation [2] (see Curve A in Fig.2). The thermophysical properties are a constant in the solid and liquid phase and vary linearly with the liquid fraction in the two phase region. The problem along with the thermophysical data and initial and boundary conditions is specified in Fig. 3a. The solidification is confined to one quarter of a corner region of dimensions 0.1m x0.1m and a convective boundary condition is assumed to prevail along the exposed edges. In the numerical run, a 21x21 uniform grid of square elements (finite element space discretization) and time steps of 0.025s and 1s are employed for the explicit and implicit scheme respectively. These choices of the time step correspond to a Fourier number in the solid phase of 0.32 (0.35 is the stability limit) and 12.7

respectively. The temperature history at x=y=0.01 m (mode 89) and x=y=0.025 m (mode 221) and the progress of solidification with time are shown in Fig.3b and 3c respectively. The results with the proposed implicit scheme agree closely with those of an explicit scheme. The total number of nonlinear iterations for the implicit scheme for 40 time steps of simulation is 213.

Solidification of a Pb-10% Sn alloy - We consider the uni-directional solidification of a Pb-10% Sn alloy initially at a uniform temperature of 350°C (greater than the liquidus temperature). The enthalpy is assumed to vary with temperature as depicted in curve B of Fig.2. The solidification is confined to a semi-infinite slab, the exposed end of which is held at 25°C. The thermophysical data and initial and boundary conditions are specified in Fig.4a. This problem was initially proposed by Poirier and Nandapurkar [13]. In the numerical run, a uniform grid of 50 linear elements of size 0.01 m (control volume space discretization) and time steps of 2 s and 10 s are employed for the explicit and implicit scheme respectively. These choices of the time step correspond to a Fourier number in the solid phase of 0.42 (0.5 is the stability limit) and 2.1 respectively. The temperature history at x=0.11 m (node 12) and the progress of the liquidus and solidus front are shown in Fig.4b and 4c respectively. The results with the proposed implicit scheme agree closely with those of an explicit scheme. The total number of nonlinear iterations for the implicit scheme for 200 time steps of simulation is 597.

Melting of gallium in a cavity in the presence of natural convection - This has been an often solved problem and involves the solution of the coupled incompressible Navier-Stokes and the energy equation. Complete details of the model, the governing equations and solution of the hydrodynamic equations can be found in Brent et al [10]. The problem along with the thermophysical data and initial and boundary conditions is specified in Fig.5a. In the numerical run, a 42 x 32 grid (control volume space discretization) and implicit time steps of 10 s are employed. Fig. 5b compares the progress of the phase front with experimental results [14]. The comparison between the predicted and experimental results can be considered to be very good. The effect of flow on the shape of the front is also clearly seen. On this problem, Brent et al. [10] using a source based method report an average of 43 iterations per time step (over 1150 time steps) and 9 minutes of CPU time on Cray-2. The proposed method, using thee same convergence criteria and inner solver, required less than 13 iterations per time step (over 1150 time steps) and the CPU requirement on the Cray-2 was reduced to 3 minutes.

References

1. Crank J. Free and Moving Boundary problems. — Clarendon Press, Oxford, 1984.
2. Kurz W., D. J. Fisher. Fundamentals of Solidification. —

Trans. Tech. Publ., Aedermannsdorf, Switzerland, 1989.
3. Bennon W. D., F. P. Incropera a. The Evolution of Macro-Segregation in Statistically Cast Binary Ingots. — Met. Trans., B, **18**, 1987, 611-612.
4. Beckermann C., R. Viskanta a. Double-diffusive Convection during Dendritic Solidification of a Binary Mixture. — PCH, **10**, 1988, 195-213.
5. Voller V. R., A. D. Brent, C. Prakash. The Modelling of Heat, Mass and Solute Transport in Solidification Systems. — Int.J.Heat Mass Transf., **32**, 1989, 1719-1731.
6. Patankar S. V. Numerical Heat Transfer and Fluid Flow. — McGraw Hill, New York, 1980.
7. Brooks A. N., T. J. Hughes. Streamline Upwind/Petrov-Galerkin Formulations for Convection Dominated Flows with Particular Emphasis on the Incompressible Navier-Stokes Equations. — Comp. Meth. Appl. Mech. Eng., **32**, 1982, 199-259.
8. Voller V. R., A. D. Brent, C. Prakash. Modelling the Mushy Region in a Binary Alloy. — Applied Mathematical Modelling, **14**, 1990, 320-326.
9. Cao Y., A. Fagiri, W. S. Chang. A Numerical Analysis of Stefan Problems for Generalized Multi-dimensional Phase Change Structures Using the Enthalpy Transforming Model. — Int. J. Heat Mass Transf.,**22**, 1989, 1289-1298.
10. Brent A. D., V. R. Voller, K. J.Reid. Enthalpy Porosity Technique for Modelling Convection-diffusion Phase Change: Application to the Melting of a Pure Metal. — Num. Heat Transf., **13**, 1988, 297-318.
11. Voller V. R., C. R. Swaminathan. A General Source Based Method for Solidification Phase Change. — Numer.Heat Transfer B. — **19B**, 1990, 175-190.
12. Swaminathan C. R., V. R. Voller. A General Enthalpy Method for Modelling Solidification Processes, submitted to Metal Trans. **B**, 1991.
13. Poirier D. R., P. Nandapurkar. Enthalpies of a Binary Alloy during Solidification, Met. Trans. B, **18B**, 1988, 245-255.
14. Gau C., R. Viskanta. Melting and Solidification of a Pure Metal on a Vertical Wall, J.Heat Transf., **108**, 1986, 174-181.

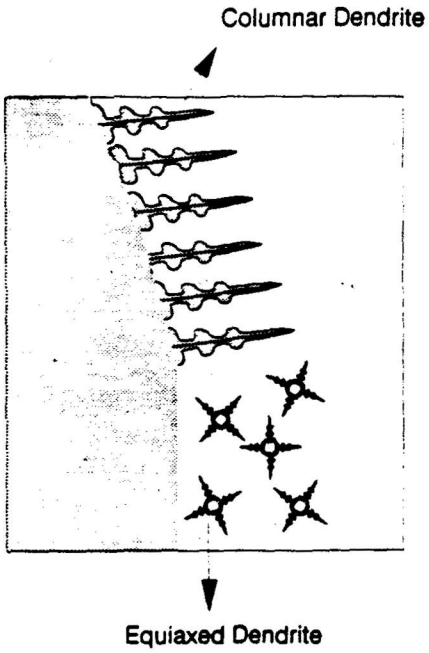

Fig.1 Schematic of the mushy region illustrating the possible morphologies.

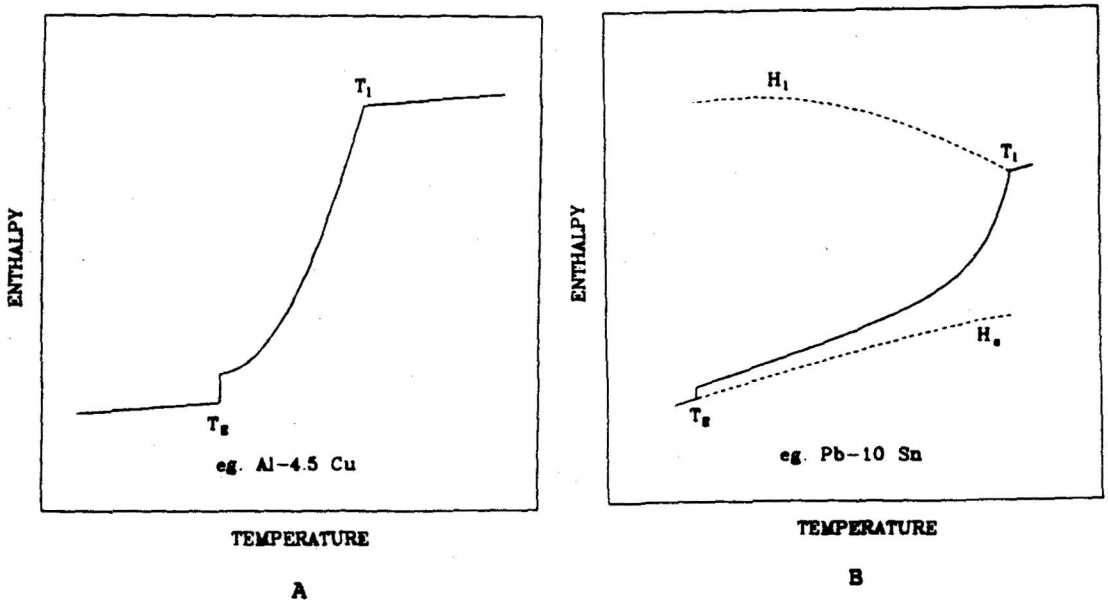

Fig.2 Enthalpy temperature relationships

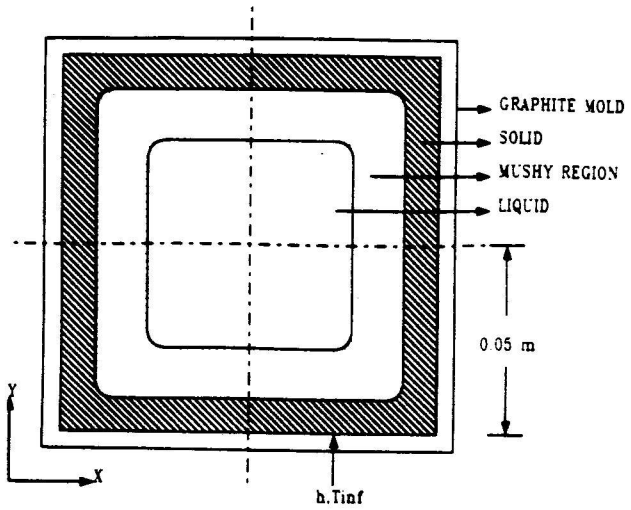

k_s	200.0 W/m K
k_l	90.0 W/m K
c_s	900.0 J/kg K
c_l	982.1 J/kg K
ρ	2800.0 kg/m^3
L	348.2 kJ/kg
T_E	821.0 K
T_l	919.0 K
T_M	933.0 K
κ	0.14
T_{ini}	969.0 K
T_{inf}	290.0 K
h	2000.0 W/m^2 K

(a)

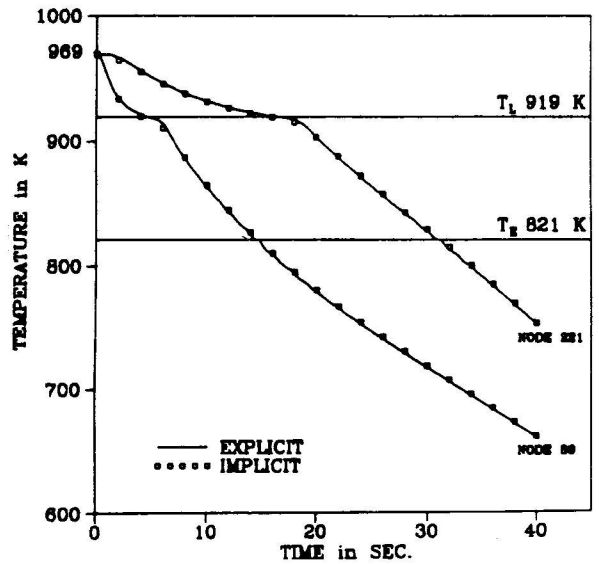

(b)

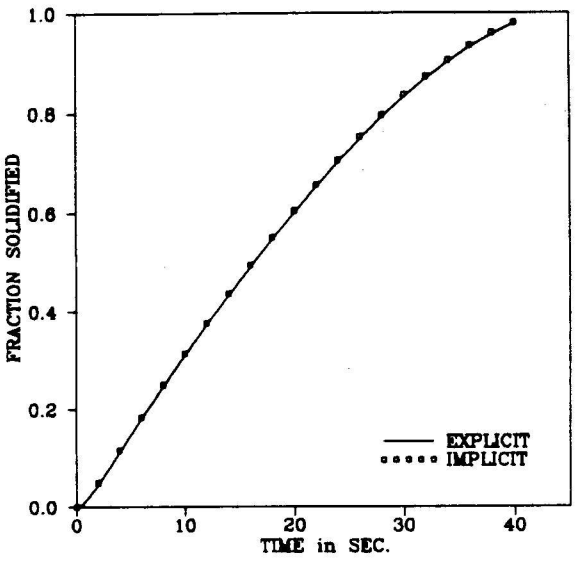

(c)

Fig.3 Two-dimensional solidification of an Al-4.5% Cu alloy: (a) Problem specification. (b) Temperature history at x = y = 0.01 m(node 89) and x = y = 0.025 m (node 221). (c) Progress of solidification with time.

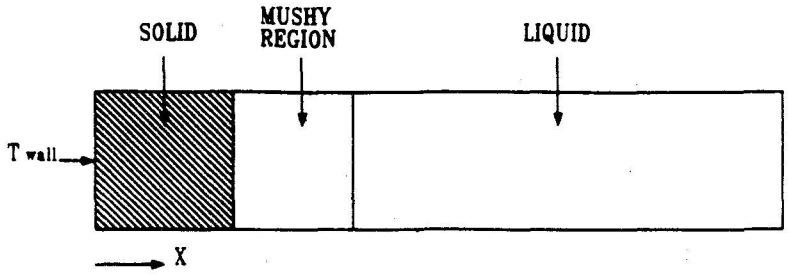

k	35.4 W/m K
c_s	159.15 J/kg K
c_l	144.75 J/kg K
ρ	10560 kg/m^3
T_L	301.5 C
T_M	183.2 C
T_{ini}	350.0 C
T_{wall}	25.0 C

Fig.4 Uni-directional solidification of an Pb-10% Sn alloy: (a) Problem specification.

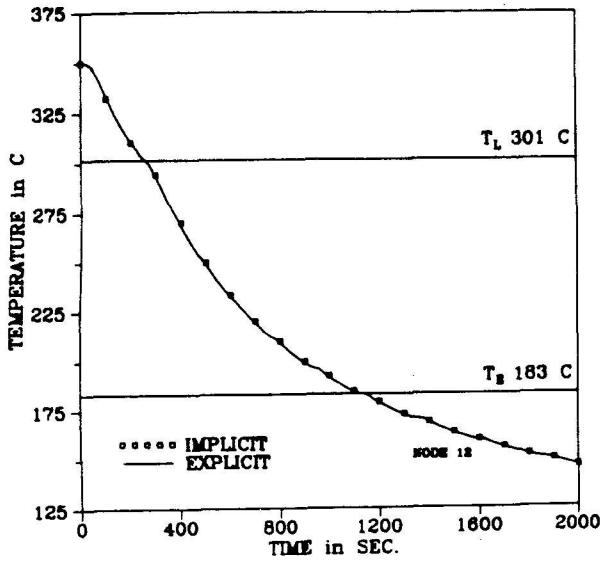

Fig.4 Uni-directional solidification of an Pb-10% Sn alloy: (b) Temperature history at x = 0.11 m (node 12).

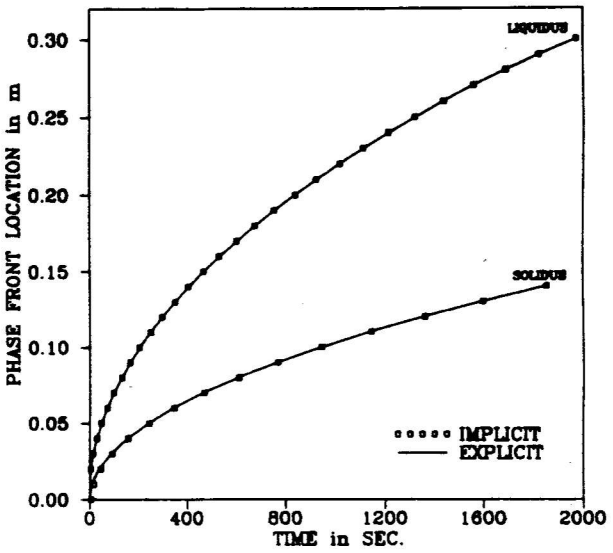

Fig.4 Uni-directional solidification of an Pb-10% Sn alloy: (c) Progress of the liquidus and solidus front with time.

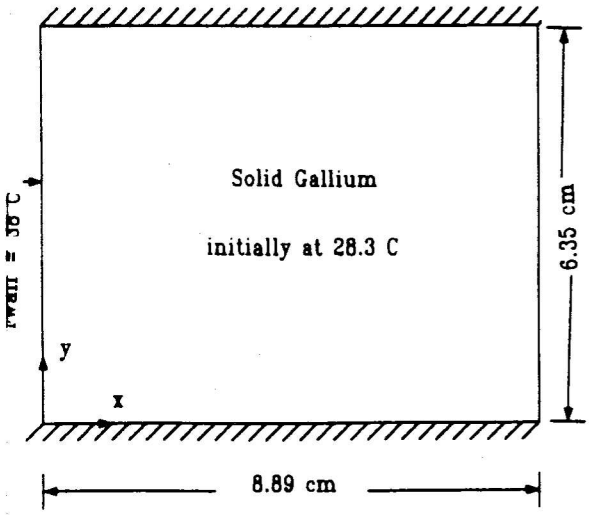

k	32.0 W/m K
c	381.5 J/kg K
μ	0.00181 kg/m s
Pr	0.0216
β	1.2×10^{-4}
ρ	6093.0 kg/m^3
L	80.16 kJ/kg
T_M	29.78 C
T_{ini}	28.3 C
T_{wall}	38.0 C

Fig.5 Melting of pure gallium in a cavity: (a) Problem specification.

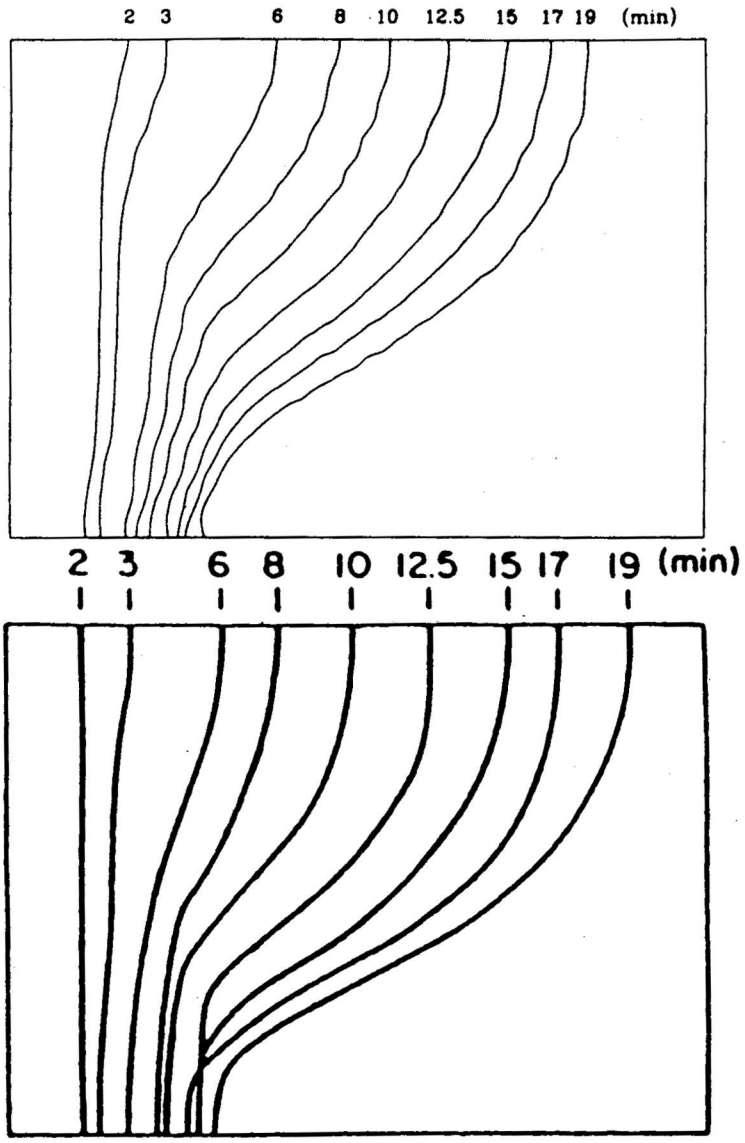

Fig.5 Melting of pure gallium in a cavity:
(b) Comparison of the numerical prediction of the progress of the phase front with experimental observations [14]